Solid–Liquid Reactions in the System Si_3N_4–β-SiAlON–$Y_3Al_5O_{12}$

Michele Wisnudel and Tseng-Ying Tien*

Materials Science and Engineering, The University of Michigan, Ann Arbor, Michigan 48109

Solid–liquid equilibria in the system Si,Al,Y/N,O were determined for the compatibility triangle bounded by the β-SiAlON solid-solution line and the compound $Y_3Al_5O_{12}$. X-ray diffraction was used to determine the crystalline phases present in the equilibrated, rapidly cooled specimens. The liquid phase was quantified with volume fraction measurements performed on scanning electron micrographs. The solid–liquid tie lines at 1650° and 1750°C were established from lattice parameters of the β-SiAlON phase and from the amount of liquid phase in equilibrium with the crystalline solid. The liquid phase was crystallized to verify the location of the starting composition.

I. Introduction

$\mathbf{S}$ILICON NITRIDE and SiAlON, silicon nitride with aluminum and oxygen replacing the silicon and nitrogen,[1] are materials currently under investigation for their application as high-temperature ceramics. The covalent bond between silicon and nitrogen provides excellent material properties, including high hardness and strength, but unfortunately prohibits densification of powder compacts. Oxide sintering agents such as Y_2O_3, Al_2O_3, and MgO aid the densification process at high sintering temperatures by forming a eutectic liquid with the silicon nitride, allowing liquid phase sintering to occur. However, this liquid phase forms a glassy grain boundary phase upon cooling and lowers the strength of the ceramic, especially at higher temperatures. Understanding the phase equilibria (or the solid–liquid equilibria) of silicon nitride–metal oxide systems provides insight into the densification processes of nitrogen ceramics and allows for the reproducible characterization of the properties of these ceramics. Silicon nitride–metal oxide systems are represented as reciprocal salt systems expressed in terms of the constituent elements, e.g., Si,M/N,O where M is a metal.[2]

Phase equilibria have been studied extensively in silicon nitride–metal oxide systems. Subsolidus phase equilibria have been investigated in the systems Si,Al/N,O[3] and Si,Y/N,O[4]. Solid–liquid equilibrium has been studied at 1750°C in the Si,Al/N,O system.[5] Combining the systems Si,Al/N,O and Si,Y/N,O gives the quasiquaternary system Si,Al,Y/N,O. Studying the phase equilibria in this system is essential to understanding the effects of adding both Y_2O_3 and Al_2O_3 as sintering aids.

The system Si,Al,Y/N,O is composed of 68 compatibility tetrahedra, but the most promising region for high-temperature ceramics is bounded by the Si_3N_4–Al_2O_3:AlN–YAG–$Y_2Si_2O_7$ compatibility tetrahedron.[6] YAG refers to the yttrium aluminum garnet, $3Y_2O_3\cdot5Al_2O_3$. Hohnke and Tien[7] studied the solid–liquid reactions in this region. They found a two-phase field over the entire Si_3N_4–$β_{60}$–YAG plane at 1550°C, with the

liquid first forming along the YAG–$β_{60}$ join. $β_{60}$ refers to the 60 equivalent percent Al-O substituted β-silicon nitride with the formula $Si_{6-x}Al_xO_xN_{8-x}$ with $x = 4$. This system was later studied by Spacie *et al.*[8] Their results differed from those of Hohnke and Tien in that the liquid was first found on the β-YAG plane at 1650°C, and the liquid phase extended from the Si_3N_4–YAG join. The focus of this research is to clarify the solid–liquid reactions in the Si_3N_4–$β_{60}$–YAG compatibility triangle at temperatures above 1550°C. Solid–liquid tie lines were established at 1650° and 1750°C from lattice parameters of the β-phase and from the amount of liquid phase in equilibrium with the crystalline solid. X-ray diffraction was used for phase identification, and scanning electron micrographs from a polished surface were used to quantify the amount of liquid phase present in the samples. The liquid phase was crystallized to verify the location of the starting composition.

II. Experimental Procedure

(1) Sample Preparation

Four compositions were prepared from the starting powders α-Si_3N_4 (Hermann C. Starck LC12), AlN (Hermann C. Starck Grade A), α-Al_2O_3, and Y_2O_3. Compositions studied are given in Table I. Oxygen content of the silicon nitride (2.0%) and aluminum nitride (1.3%) powders were taken into account in computing the compositions. These compositions were mixed by hand with an agate mortar and pestle with isopropyl alcohol. Dried mixtures were pressed into pellets and isostatically pressed under a pressure of 300 MPa. All of the specimens were put in BN-packed graphite crucibles and fired in a graphite-resistant furnace under static nitrogen of 1 atm pressure. The samples were heat treated at 1650° and 1750°C. Samples were soaked for 24 h at a temperature sufficient to ensure equilibrium. Specimens used for phase analysis had less than 2% weight loss after firing at 1650°C and 3% weight loss after firing at 1750°C.

(2) Phase Identification

Specimens were analyzed using X-ray diffraction with Cu$Kα$. All heat-treated samples contained only two phases, β-SiAlON and liquid. The glassy phase was apparent from the X-ray data because of increased background intensity. β-SiAlON has a hexagonal structure and it was identified with X-ray data. Lattice parameter calculations were performed to determine the amount of Al in the β-SiAlON phase. A computer program was utilized to carry out these calculations.[9] The β-SiAlON peak angles were input with their corresponding planes so that the lattice parameters, a and c values of the β-SiAlON hexagonal unit cell, could be given as output. The β-SiAlON peaks used for identification include [200], [210], [300], [310], [301], [221], [311], and [320]. The generated lattice parameters were compared with β-silicon nitride and $β_{60}$ lattice parameters to determine x in the SiAlON formula, $Si_{6-x}Al_xO_xN_{8-x}$. It has been shown that the lattice parameters of β-SiAlON vary linearly with x.[10] The x values were converted to weight percent AlN:Al_2O_3 and are plotted on the Si_3N_4–$β_{60}$–YAG compatibility triangle. For example, $β_{60}$ can be expressed either with the formula ($x = 4$) $Si_2Al_4O_4N_4$ or as a combination of the starting materials required to produce this

Table I. Sample Compositions with Relative Amounts of Starting Powders

Sample ID	Compositions (wt%)	Si_3N_4	Y_2O_3	Al_2O_3	AlN
SY-19	$90\,\beta_{10}/10$ YAG	79.938	5.706	7.948	5.769
SY-20	$90\,\beta_{23}/10$ YAG	66.522	5.706	17.973	9.269
SY-21	$90\,\beta_{36}/10$ YAG	53.106	5.706	28.002	12.764
SY-22	$90\,\beta_{49}/10$ YAG	39.690	5.706	38.038	16.25

formula. β_{60} can be written as $\frac{2}{3}Si_3N_4 + \frac{4}{3}AlN{:}Al_2O_3$, and the weight percent of $AlN{:}Al_2O_3$ can be calculated. β_{60} contains 67.1 wt% $AlN{:}Al_2O_3$. Similarly the $AlN{:}Al_2O_3$ weight percents of the individual β-phases can be calculated. Once the weight percents of $AlN{:}Al_2O_3$ are known, lines can be drawn connecting the position of the starting composition on the compatibility triangle to the weight percent of $AlN{:}Al_2O_3$ on the Si_3N_4–$Si_2Al_4O_4N_4$ join. The lattice parameters of specimens after firing were determined and compared with the standard values. The results are given in Table II.

(3) Liquid Phase Quantification

Samples were polished for scanning electron microscopy studies. Two phases were apparent from SEM micrographs: silicon nitride grains and the liquid phase surrounding the grains. The volume fraction of liquid phase present in the specimens was quantified by measuring the volume of liquid phase apparent from the SEM micrographs. The point count method used to calculate the volume fraction of this liquid phase is described in Underwood.[11] Micrographs of the same magnification (10 k) and same area were used for the measurements. A grid was placed over the micrographs and the number of grid intersections which covered the liquid phase area were totaled. This number was divided by the total number of grid points to calculate the liquid phase volume fraction. The number of grid points used to calculate the volume fractions was deciphered in order to establish a 10% confidence interval.

The liquid phase volume fractions were converted to weight fractions using the following equation:

$$X_W = \frac{X_{vl}\rho_l}{X_{vl}\rho_l 1 + X_{v\beta}\rho_\beta} \quad (1)$$

X_W is the weight fraction of the liquid phase, and X_{vl} and $X_{v\beta}$ are the volume fractions of liquid and β phases. ρ_l and ρ_β are the densities of the liquid and β-phases. The density of the liquid phase was estimated using Y-Si-Al-O-N glass density results published by Messier.[12]

The value of 3.92 g/cm³ was used for the glass density. The density of each β-SiAlON was calculated using the equation

$$\rho = \frac{280.5666 + 0.8887x}{[(7.6059 + 0.0273x)^2(2.9108 + 0.0244x)](0.866)}\frac{g}{cm^3} \quad (2)$$

The variable x is the same as that seen in the β-SiAlON formula, $Si_{6-x}Al_xO_xN_{8-x}$. Once the weight fraction of the liquid phase is known, the liquidus location can be determined using

the lever rule. The results of these measurements are given in Table III.

(4) Liquid Phase Crystallization

Heat-treated samples were annealed in the graphite-resistant furnace under static nitrogen of 1 atm pressure. Samples were held at 1400°C for 24 h, since it has been shown that nearly complete crystallization of the liquid phase can occur at this temperature and time duration. X-ray analysis was performed on samples to determine phases. Two phases, β-phase and YAG, were apparent in the samples. Lattice parameter calculations were performed on the β-phases and were compared to results from nonannealed samples. It is apparent that there was a compositional change during firing. The lattice parameters and the x-values of the solid solutions are given in Table IV.

III. Results and Discussion

Samples were sintered at 1650° and 1750°C, and phases were analyzed using X-ray diffraction. The equilibrium and nonequilibrium phases were detected; two types of nonequilibrium phases were identified. The first type of nonequilibrium phase is one that occurs off the plane of the Si_3N_4–β-SiAlON–YAG compatibility plane. These types of phases include yttrium silicates and SiAlON polytypoids.[13] These phases occur primarily because of the difficulty in composition control and processing. The second type of nonequilibrium phase detected is YAG. Samples sintered at 1650°C contained crystalline YAG when the sintering times were short and the cooling rates were slow. However, samples held at both 1650° and 1750°C for 24 h contained only β-SiAlON and a liquid phase. Equilibrium was

Table III. Results of Liquid Phase Quantification

Sample ID	β-SiAlON density (g/cm³)	Volume fraction, liquid phase	Weight fraction, liquid phase
1650°C			
SY-19	3.173	0.127	0.152
SY-20	3.134	0.134	0.162
SY-21	3.098	0.135	0.165
SY-22	3.064	0.136	0.167
1750°C			
SY-19	3.163	0.121	0.145
SY-20	3.122	0.136	0.165
SY-21	3.094	0.139	0.169
SY-22	3.064	0.142	0.175

Table II. β-SiAlON Lattice Parameters after Sintering

Sample ID	a (Å)	c (Å)	x	Weight percent $AlN{:}Al_2O_3$
1650°C				
SY-19	7.617	2.920	0.55	0.093
SY-20	7.645	2.946	1.55	0.262
SY-21	7.669	2.967	2.50	0.421
SY-22	7.695	2.990	3.40	0.571
1750°C				
SY-19	7.624	2.926	0.80	0.135
SY-20	7.652	2.953	1.85	0.312
SY-21	7.673	2.970	2.60	0.438
SY-22	7.696	2.990	3.40	0.572

Table IV. β-SiAlON Lattice Parameters after Crystallization

Sample ID	a (Å)	c (Å)	x	Weight percent $AlN{:}Al_2O_3$
1650°C				
SY-19	7.624	2.930	0.80	0.135
SY-20	7.651	2.951	1.75	0.294
SY-21	7.673	2.972	2.60	0.438
SY-22	7.695	2.991	3.45	0.579
1750°C				
SY-19	7.629	2.933	1.05	0.178
SY-20	7.652	2.952	1.85	0.312
SY-21	7.674	2.972	2.65	0.446
SY-22	7.697	2.991	3.50	0.587

assumed to occur when phases remained consistent through extended sintering times. The equilibrium phases are β-SiAlON and liquid. Only those samples considered to be at equilibrium were further analyzed.

Lattice parameter measurements were calculated on those samples which contained β-SiAlON and a liquid phase. The lattice parameter values of the individual β-phases were compared to Si_3N_4 and $β_{60}$ lattice parameters. The amount of solid solution was determined for each composition at 1650° and 1750°C, and these data are summarized in Table II. This information can also be visualized on the Si_3N_4–β-SiAlON–YAG compatibility triangles. Diagrams were drawn with weight percent $AlN:Al_2O_3$ as the scale along the Si_3N_4–$β_{60}$ join. Lines connect the position of the prepared composition with the corresponding amount of solid solution along the Si_3N_4–$β_{60}$ join. It is important to note the shift in weight percent of $AlN:Al_2O_3$, or the increasing Al solubility in the Si_3N_4, with increasing temperature.

Scanning electron microscopy was performed on samples polished to 0.1 mm. Liquid volume fractions were calculated on the micrographs using the point count method. Densities were calculated for the β-phases, and the liquid volume fractions were converted to weight fractions. The results are listed in Table III. The liquid weight fractions are approximately 16% for both the samples sintered at 1650° and 1750°C. In Fig. 1, the tie lines are extended to include the liquid phase information.

It appears from the diagrams that the liquidus region extends from the Si_3N_4–YAG join; however, these tie lines were drawn connecting the weight percent $AlN:Al_2O_3$ of each β-phase with

the starting composition of each sample. The starting compositions may shift during heat treatment, so a second heat treatment was performed to verify the starting composition location.

Samples were annealed to crystallize the liquid phase. Two phases were present in these samples, β-phase and YAG. Lattice parameter measurements were performed to determine the amount of Al in the β-phase. These results are tabulated in Table IV. Tie lines were drawn connecting the amount of Al in solid solution along the Si_3N_4–$β_{60}$ join to YAG, the apex of the Si_3N_4–$β_{60}$–YAG compatibility triangle in Fig. 1. The amount of solid solution in each of the samples appears to increase after crystallization. It is apparent from Fig. 1 that the location of what was considered to be the original composition shifted during sintering. Since the β-phase–YAG tie lines do not contain the starting composition point, the location of the starting composition is changed during sintering. SiO gas evaporates from the samples, especially at higher sintering temperatures. This is apparent from the sintered sample weight losses. The weight losses for samples sintered at 1650°C were about 2%, but for the samples sintered at 1750°C, weight losses were 3%, causing the apparent shift in starting composition. New tie lines are drawn to compensate for this shift. Tie lines connect the original β-phase lattice parameters to the approximate starting composition (on the β-phase-YAG tie line) and continue to the liquidus location, since the relative weight fractions of β-phase and liquid phase are known from the original heat treatments. Figure 2 shows a combined diagram with 1550°, 1650°, and 1750°C isotherms. The approximated liquid phase regions are depicted in Fig. 3. The liquid region extends further into the compatibility triangle at 1750°C. These results are consistent with those seen by Bonnell *et al.*[14] The results differ, however, from those seen by Spacie *et al.*[8] These researchers show the liquid phase extending from the YAG–Si_3N_4 join at 1700°C. This phenomenon is similar to what was observed prior to accounting for the shift in starting composition. Since weight losses occur in the sintered samples, shifts in the starting composition must be taken into account.

IV. Conclusion

The solid–liquid equilibrium isotherms have been constructed for the system Si_3N_4–SiAlON–YAG at 1650° and 1750°C. The liquid phase extends from the YAG–β-SiAlON join and increases with increasing temperature. Phase equilibrium and starting composition compensation are two necessary factors in determining these isotherms. The methods of using X-ray diffraction for phase identification and scanning electron microscopy for volume fraction determinations have been effective in analyzing these solid–liquid reactions.
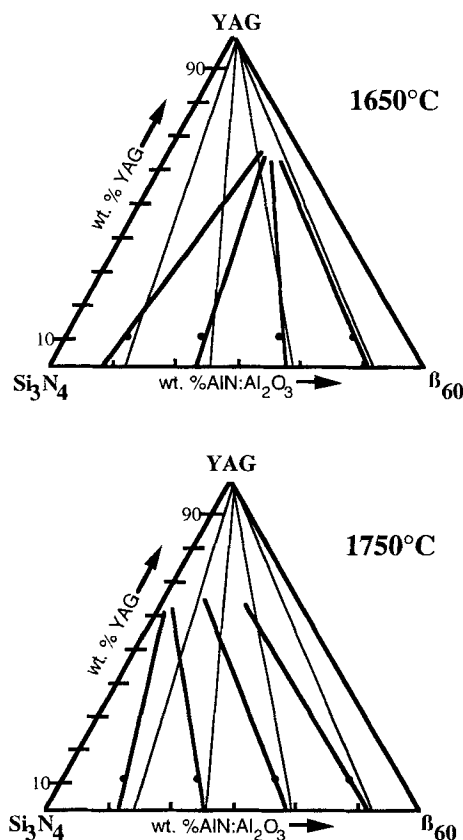
Fig. 1. The dots represent the original prepared starting compositions. The thick lines represent the tie lines which were drawn after the first heat treatment. These tie lines connect the weight percent $AlN:Al_2O_3$ of each β-phase to the starting composition. The length of the tie line was determined using the lever rule, since relative amounts of liquid and β-phases were determined. The thin lines represent the tie lines which were drawn after the samples were annealed. These tie lines connect the weight percent $AlN:Al_2O_3$ of each β-phase to YAG, the apex of the compatibility triangle. These diagrams show that the starting compositions are shifting during heat treatment, especially at 1750°C.
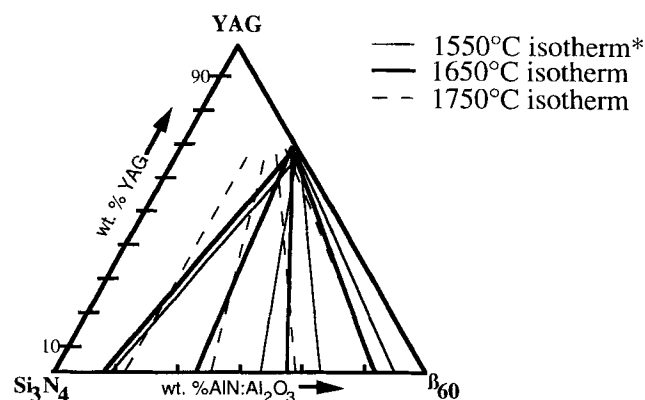
Fig. 2. New tie lines are drawn connecting the weight percent AlN: Al_2O_3 of the original β-phase to the approximate position of the starting composition on the Si_3N_4–YAG tie line. The lengths of the tie lines were determined from the relative amounts of liquid and β-phase after heat treatments at 1650° and 1750°C. (*Hohnke and Tien,[7] p. 103.)
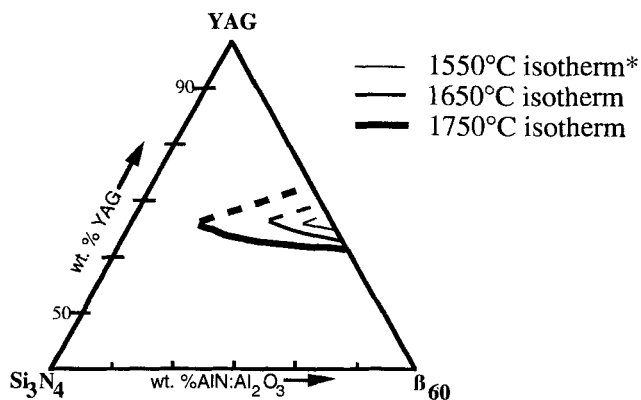
Fig. 3. Approximated liquid phase regions for 1550°, 1650°, and 1750°C. The continuous lines represent experimentally determined isotherms, and the dashed lines represent estimated upper bounds to the liquid phase region. (*Hohnke and Tien,[7] p. 103.)

References

[1]K. H. Jack and W. J. Wilson, "Ceramics Based on the Si-Al-N-O and Related Systems," *Nature (London) Phys. Sci.*, **238** [80] 28–29 (1972).

[2]L. J. Gauckler, H. L. Lukas, and G. Petzow, "Contribution to the Phase Diagram Si₃N₄-AlN-Al₂O₃-SiO₂," *J. Am. Ceram. Soc.*, **58** [7–8] 346–47 (1975).

[3]L. J. Gauckler and G. Petzow, "Representation of Multi-component Silicon Nitride Based Systems"; pp. 41–62 in *Progress in Nitrogen Ceramics*. Edited by F. Riley. Noordhoff, Leyden, Netherlands, 1977.

[4]L. J. Gauckler, H. Hohnke, and T. Y. Tien, "The System Si₃N₄-SiO₂-Y₂O₃," *J. Am. Ceram. Soc.*, **63** [1–2] 35–37 (1980).

[5]I. K. Naik, L. J. Gauckler, and T. Y. Tien, "Solid–Liquid Equilibria in the System Si₃N₄-AlN-SiO₂-Al₂O₃," *J. Am. Ceram. Soc.*, **61** [7–8] 332–35 (1978).

[6]W. Y. Sun, T. Y. Tien, and T. S. Yen, "Subsolidus Phase Relationships in Part of the System S,Al,Y/N,O: The System Si₃N₄-AlN-YN-Al₂O₃-Y₂O₃," *J. Am. Ceram. Soc.*, **74** [11] 2753–58 (1991).

[7]H. Hohnke and T. Y. Tien, "Solid–Liquid Reaction in Part of the System Si,Y/N,O"; pp. 101–10 in *Progress in Nitrogen Ceramics*. Edited by F. L. Riley. Martinus Nijhoff, The Hague, Netherlands, 1983.

[8]C. J. Spacie, N. S. Jameel, and D. P. Thompson, "The Fabrication of Two-Phase β-SiAlON–YAG Ceramics"; see Ref. 7, pp. 343–49.

[9]M. H. Mueller and L. Heaton, "Determination of Lattice Parameter with the Aid of a Computer," Final Report of Metallurgy Program 4.1.8, Report No. ANL-5975; pp. 67–77. Argonne National Laboratory, Argonne, IL, 1959.

[10]L. J. Gauckler, J. Weiss, T. Y. Tien, and G. Petzow, "Insolubility of Mg in β-Si₃N₄ in the System Al,Mg,Si/N,O," *J. Am. Ceram. Soc.*, **61** [9–10] 397–98 (1978).

[11]E. Underwood, *Quantitative Stereology*. Addison-Wesley, Reading, MA, 1970.

[12]D. Messier, "Preparation Crystallization of Si-Y-Al-O-N Glasses," *Ceram. Eng. Sci. Proc.*, **3** [9–10] 565–76 (1982).

[13]L. J. Gauckler, "Phase Equilibria Studies in the System Si,Al/N,O and Si,Al,Be/N,O"; Sc.D. Thesis. University of Stuttgart, Federal Republic of Germany, 1976.

[14]D. A. Bonnell, M. Ruhle, and T. Y. Tien, "Redistribution of Aluminum Ions during Processing of SiAlON Ceramics," *J. Am. Ceram. Soc.*, **69** [8] 623–27 (1986). □